International Conference on Applied Energy 2020
Dec. 1 - Dec. 10, 2020, Bangkok / Virtual
Paper ID: 460

Optimal switch model for Load Frequency Control applied to a multi-microgrid using Energy Storage System

M.W. Siti[*1], N.T. Nsilulu[2,4], D.H. Tungadio [3], R.C. Bansal[4], R. Naidoo[2], R. Tiako[5], T. Ratau[1]

[1] Department of Electrical Engineering, Tshwane University of Technology, Pretoria, South Africa
[2]Department of Electrical, Electronic and Computer Engineering, University of Pretoria, South Africa
[4]Department of Electrical and Electronic Engineering Science, University of Johannesburg, South Africa
[4]Department of Electrical Engineering, University of Sharjah, Sharjah, United Arab Emirates
[5]Department of Electrical Engineering, University of KwaZulu-Natal, Durban, South Africa
(Corresponding Author: ntmbungu@ieee.org)

ABSTRACT

The control of active power and frequency in a network to regain its stability is referred to as load frequency control (LFC). The area control error (ACE) is a combinatorial model between the tie-line in the interconnected system and the deviations of its frequency. In terms of network control and network balancing, the ACE is forced to be close to zero to achieve generation and load balance. This paper presents an investigation into load frequency control with an optimal control theory, using an energy storage system (ESS). The system consists of two tie-lines connected between the two areas, and each one is made up of a synchronous generator, renewable energy sources, ESS and load. Control strategies are developed based on the optimal control theories, frequency deviation and ACE, with the aim to regulate the ESS output. The performance verification is done by a comparative assessment of the optimal control strategy. The effectiveness of the frequency control strategies is measured through simulation.

Keywords: renewable, Frequency Control, advanced energy technologies,

1. INTRODUCTION

Conventional energy generation from thermal and other non-renewable sources has contributed to climate change. This can be addressed by incorporating renewable energy (RE) [1]. Microgrids are low and medium voltage grids which interconnect distributed generation (DG) with different sources and ESS connected by different feeders with the loads [2]. A microgrid typically supplies 10 MVA maximum load capacity [1]. A microgrid can be defined as a structure in which the tie-lines are connected to different sources, for example, the combination of renewable energy with the diesel generator. This type of system can be found at both the medium and low level. The introduction of the control requires proper configuration to enable network management under different circumstances. In the power system analysis, the control of active power is referred to as load frequency control. In most cases where the areas are interconnected, the basic assumption is that each area must have a system to control its generation.

The energy storage system plays an essential role in the introduction of renewable energy. It is an integral part of the system and can provide fast active power compensation. The energy storage system also can enhance the load frequency control performance. Regarding mitigating the dynamics which are introduced by non-dispatchable variable generation, the energy storage system provides a better response [3]. The storage facilities in the microgrids network also possess benefits due to its dynamic to bring the structure into the stabilization process by load levelling, spinning reserve, area regulation, and the improvement of the power factor [4]. In different analyses of load frequency control, the ESS has been used to provides power compensation [5].

In this paper, the introduction of the new concept is a model application of the combinatorial solution to control the different areas connected by the tie-line as ESS switched modes (charge and discharge) of the battery, which is described by switched constraints. The power system presented in this paper consists of two main areas; each area is made up of a diesel generator, a

Selection and peer-review under responsibility of the scientific committee of the 12th Int. Conf. on Applied Energy (ICAE2020).

renewable energy source, the PV, wind generation, energy storage system, and its load.

The configuration of the power system is shown in Figures 1 and 2. The control strategies are developed regarding the two parameters, the frequency deviation and the ACE, to regulate the ESS output during the two modes (charge and discharge) by the switching technique of its constraints. The main contributions of

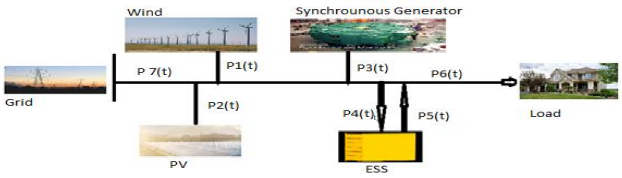

Fig. 1. Power system configuration of micro grid

Fig. 2. Power system configuration with multiple areas or multi-micro gridmicrogrid system

this paper are:

- The regulation of the storage system by the switching mode algorithm.
- The improvement in frequency deviation reduction.

Problem Statement

2.1 Overall Structure of Microgrid

As shown in Fig. 1, the proposed microgrid system is a combination of a diesel generator, a PV, the wind generation, ESS and the load. Regarding the control strategies, the charging and discharging of the ESS are unpermitted, resulting in a robust and more practical model.

2.*2 Synchronous Generator System*

Standby synchronous generator works as a back-up plan to supply deficit power to the microgrid system to meet its load demand. Where the power flow from the grid $P_7(t)$ must be superior to $P_6(7)$. Small loads can use the diesel generator, but for large load demand, the application of turbine-driven generator is required. The selection of the synchronous generator consists of a speed governor and turbine. Their transfer function can be expressed by [4, 6]:

$$G_G(s)=\frac{\Delta P_3(s)}{\Delta P_g(s)}=\frac{K_g}{1+sT_g} \quad (1)$$

$$G_T(s)=\frac{\Delta P_m(s)}{\Delta P_3(s)}=\frac{K_T}{1+sT_T} \quad (2)$$

where T_g and T_T represent the time constant of governor and turbine respectively, and P_3 represents the power flow in the PV generation at any time of the control horizon. The selected value of governor gain constant (*Kg*) and turbine gain constant (K_T) as two essential parameters in the model is set to 1.0. The range of the value selected for the speed regulation is between 5 to 6% of full [7].

2.3 Wind Power Generation

The selection of the standard deviation for wind generation is used by in [8] as the simulated function:

$$dp_{P_1}=0.8\sqrt{P_1} \quad (3)$$

Eq. 3 is derived by Matlab Simulink as a random output fluctuation.

2.4 Solar Photovoltaic Model

The configuration of the PV involves cells connected in series as well as in parallel to achieve better output voltage. The number of cells is calculated considering the current drawn by the load. Another critical parameter is solar radiation. The maximum power tracking another component apply to increase the solar radiation effectively to obtain the maximum radiation. Eq. (4) is used to determine the output power of the PV.

$$P_{PV}=\eta S\varphi\left[-0.005\left(T_a+25\right)\right] \quad (4)$$

In this paper, the power flow from the PV is represented by $P_3(t)$, as applied by Eq. (4), and η represents the conversion efficiency of the PV array, *S* represents the area of PV array (m^2), φ is solar irradiation (kW/m^2), and Ta is ambient temperature expressed in ^oC. The PV transfer function of the PV system can be represented by a linear first-order lag [9],

$$G_{P_3}(s)=\frac{\Delta P_{P_3}}{\Delta\varphi}=\frac{K_{P_3}}{1+sT_{P_3}} \quad (5)$$

where K_{P_3} is the gain constant and T_{P_3} is the time constant.

2.5 Energy Storage System

The dynamics of the model of the ESS can be Expressed by

$$Soc(t+1) = SOC(t) + n_C P_4(t) - n_d^{-1} P_5(t) \quad (6)$$

Where $P_4(t)$ and $P_5(t)$ represent power flow during charging and discharging respectively. $\mathrm{SOC}(t)$ is the state of charge, *t* is sampling time, η_c and η_d are, charging and discharging efficiency, respectively. To determine proportional to the battery dynamic (charging and discharging) of the current to establish the switching mode of ESS on the application of the optimal control, the state of charge (SOC) at a given sample is expressed in time series as [10-14]:

$$SOC(t) = SOC + n_c \sum_{t=0}^{N} P_4(t) - n_d^{-1} \sum_{t=0}^{N} P_5(t) \quad (7)$$

The ESS dynamic has the ability on the active and reactive power output as presented by Eq. 7, with reference on the charging and discharging process its switching frequency can move above the kHz range. Its main applications are harmonic cancellation, load levelling and output voltage control. And It also plays a vital role in providing additional damping to the power system network swings to enhance transient and dynamic stability [15]. Its transfer function can be taken as first-order lag.

$$G_{ESS}(s) = \frac{\Delta(P_4 - P_5)}{\Delta\omega} = \frac{K_{ESS}}{1 + sT_{ESS}} \quad (8)$$

Where K_{ESS} and T_{ESS} represent the gain constant and time constant, respectively.

2. SYSTEM MODELLING AND DESIGN

The interconnected power system, which is combined with more than one area, presents many advantages in power system analysis; the system will be more reliable in supply as illustrated by Figs. 1 and 2. The total power flows into the two areas, taking into consideration the tie-line deviation, applying the load equation to determine the total amount of energy received by the load is represented by Eq. (9).

$$P_1(t) + P_2(t) + P_3(t) + P_4(t) - P_5(t) = P_6(t) \quad (9)$$

where $P_6(t)$ is the receiving power or the total power generated by different sources. Two important parameters are used to determine the electrical energy sent through the main bus by each area; the full power and the total power demand (P_D). This can be expressed as:

$$\Delta P_e = P_6(t) - P_D \quad (10)$$

In the fundamental relation between the active power and the frequency, the frequency deviation through any area can be expressed as:

$$\Delta\omega = \frac{\Delta P_e}{K_{sys}} \quad (11)$$

where $\mathrm{K}_{\mathrm{sys}}$ represents system frequency characteristic constant of any area in the network. When the network encounters power deviation, there is a time delay for the frequency to vary. This scenario introduces time delays, where the transfer function of the system frequency varies per unit of deviation, and it is expressed as:

$$Gsys(s) = \frac{\Delta\omega}{P_6 - P_D} = \frac{1}{K_{sys}(1 + sT_{sys})} = \frac{1}{D + Ms} \quad (12)$$

where *M* and *D* represent the equivalent inertia constant and damping constant of the area, respectively.

Fig. 3 represents the structure on the two areas interconnected by a tie line where the frequency deviation and the ACE are optimized. The tie-line power deviation (ΔP_{TL}), the synchronizing power coefficient (P_S), $\Delta\omega_1$ and $\Delta\omega_2$ are frequency deviations in areas 1 and 2. And Eq. 13 determine the tie-line deviation.

$$\Delta P_{TL} = P_S\left(\int \Delta\omega_1 dt - \int \Delta\omega_2 dt\right) \quad (13)$$

3.1 Objective Function

The area control error is an essential factor in the model, which must be optimized, to achieve that the frequency deviation between the tie must be equals to zero. In two areas model, as presented in this paper, it also is essential to design the model to optimize and to consider the ESS constraints.

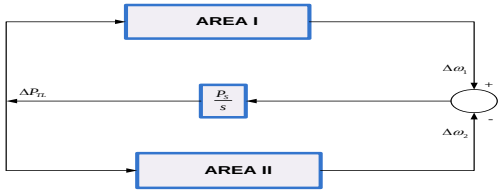

Fig. 3: Modelling of the tie line [16]

$$ACE_i \sum_{j=1}^{t} \Delta P_{ij} + B_i \Delta \omega_i \quad (14)$$

where *B* represents the frequency bias factor for *i*th in the area. Fig. 4 shows the block diagram in Simulink of two interconnected area power systems. In this model, to optimize Eq. (14), the ESS may be controlled by either the frequency deviation or ACE.

3.1 Constraints

The constraints are defined as parameters to the ESS dynamics which has an impact of the feedback of the frequency the deviation as on ACE, the minimum and the maximum capacity of the ESS is defined as a constant value. It can be expressed by the following constraint [15, 16]:

$$SOC^{\min} \le SOC(k) \le SOC^{\max} \quad (15)$$

Eq. (15) can be translated into equation (16), in which case, the lower limit for the SOC of the battery bank cannot be exceeded at the time of discharge $(SOC_{\min})$. This may be expressed as follows [17-24]:

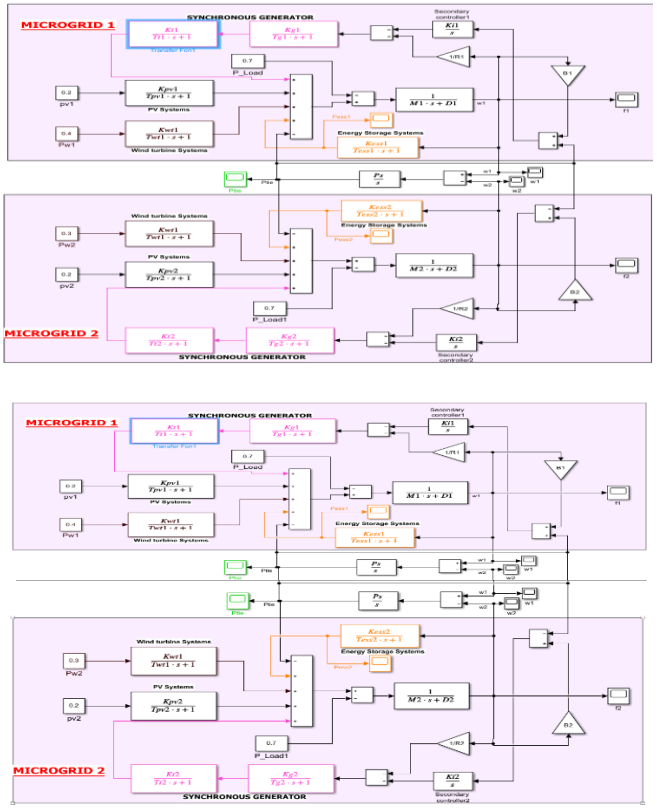

Fig. 4. An interconnected power system with two areas.

$$SOC^{\min} = (1 - DOD).SOC^{\max} \quad (16)$$

where *DOD* is the depth of discharge expressed as a percentage.

Eq. (17) considers the law of supply and demand and ensures that of the contribution of each source in the model.

$$P_1(t) \ge 0;\ P_5(t) \ge 0;\ P_6(t) \ge 0; \quad (17)$$

Each given energy source, *i*, is constrained by minimum and maximum values as specified in Eq. (17):

$$P_i^{\min}(t) \le P_i(t) \le P_i^{\max}(t) \quad (18)$$

3. RESULTS AND DISCUSSIONS

Table I presents simulations parameters of the system model. The results presented in Fig. 5, show the need to optimize the $\Delta\omega$ and ACE feedback by using the switching model of ESS. The parameters output of the model are reduced; this can be seen with Fig. 6 and Table II, which present the signal error reduction of the frequency deviation as well as the ACE. The second analysis of the interconnected network is done to shown robustness of the model during the different uncertainties such as the frequency deviation, output power of the energy storage system and the deviation of the power flowing from different tie lines when the interconnected network is under uncertainties. The implementation of the switching technique model and

Table I: Area parameter values

Parameters	Definition	Area1	Area2
$R(pu)$	Speed regulation	0.005	0.004
$T_g(s)$	Governor time constant	0.1	0.1
$T_T(S)$	Turbine time constant	0.4	0.4
$T_{PV}(s)$	Solar PV time constant	1.5	1.4
$T_{ESS}(s)$	ESS time constant	0.1	0.1
KI	Integral constant	5	7
$B(pu)$	Frequency biasing factor	10	12.5
M (pu)	Inertia constant	0.8	0.7
D (pu)	Damping constant	0.02	0.03

the results presented from Fig. 6 show an improvement

in frequency deviation reduction and the tie-line when optimal control used to the ACE with the feedback to ESS compare to the feedback deviation of the frequency. This can also be seen in Table II. where the error signal is

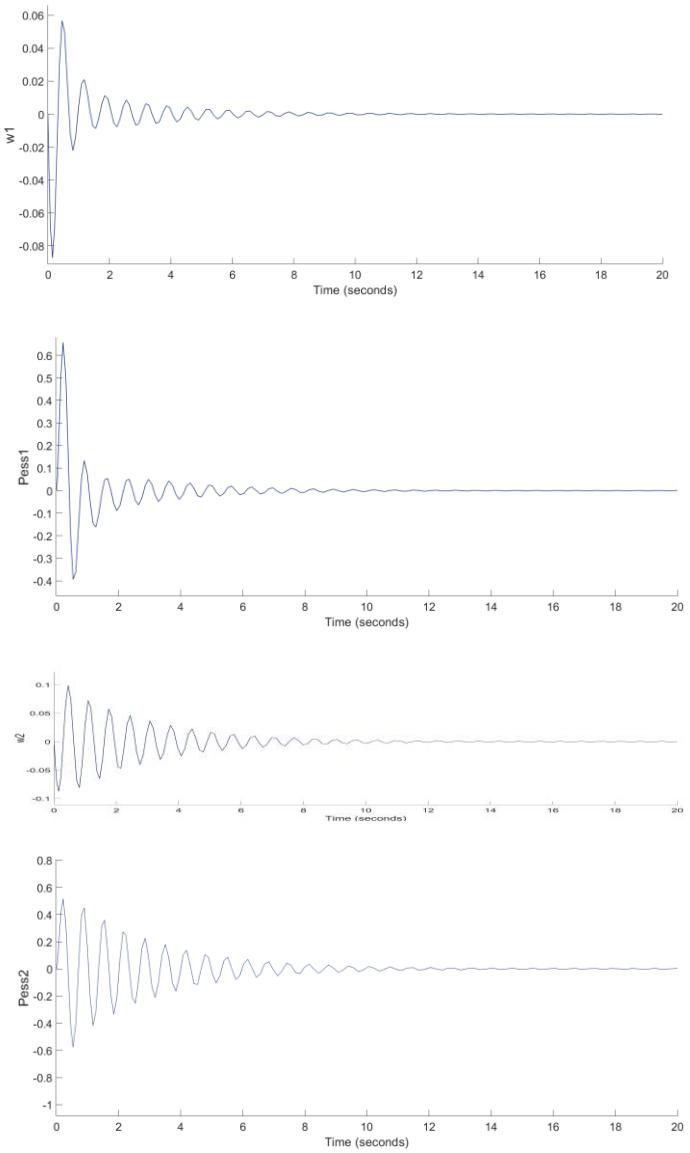

Fig. 5. The parameters output for Δω feedback using ESS control

reduced during the application of the optimal control using Eq. (14) and its constraint applications.

The application of the optimal control using the ESS switching model as the feedback to ACE and Δω shows a complete reduction of the signal error, as shown in Table II. This can be seen with two areas and the power deviation between the two areas. Also in Table II, where switching model is used of the ACE feedback to ESS show a better reduction of the error compared to frequency deviation, which relies on the constraints of

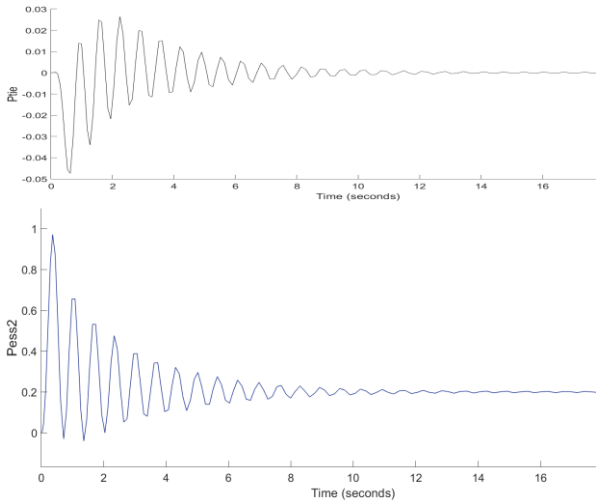

Fig. 6. The parameters output for ACE feedback using ESS control

Table II: Frequency and tie-line deviation

Error Signal	$\Delta\omega$ Feedback	ACE Feedback
Frequency deviation area 1	2.223×10^{-6}	1.024×10^{-7}
Frequency deviation area 2	2.533×10^{-8}	4.421×10^{-9}
Power deviation Line 1-2	1.442×10^{-7}	1.213×10^{-9}

the model and the boundaries to improve the ACE feedback to ESS by using Eqs. (15-17).

4. CONCLUSION

Optimal control and the ESS switching model are applied on a power system interconnected system where load frequency is the control to achieve the frequency deviation to be close to zero and keep the interconnected system in a stable condition during the load deviation. The output control of the different parameters such as frequency and tie-line deviation are analyzed using an objective function (with its constraints). The error signal was completely reduced using this model. To achieve better results, a mathematical model of a switching model with optimal control was used to simplify the simulation by using the objective function, which is defined in the paper. The step of the load change was used as one of the steps during the optimization process. With the switching optimal model process, it is observed that the regulation

of the ACE to zero is applicable for the load frequency control in the interconnected system.

References

[1] Siti, M. W., Tungadio, D. H., Sun, Y., et al.: Optimal frequency deviations control in microgrid interconnected systems. IET Renewable Power Generation, 2019, **13**, (13), pp. 2376 – 2382.

[2] N. T. Mbungu, R. M. Naidoo, R. C. Bansal, V. Vahidinasab, "Overview of the optimal smart energy coordination for microgrid applications," IEEE Access, 2019, **7**, pp. 163063–163084.

[3] Levron Y., Guerrero J. M., and Beck Y.: Optimal Power Flow in Microgrids with Energy Storage. *Power Syst. IEEE Trans.*, 2013, **28**, (3), pp. 3226-3234.

[4] Ahmadi A., and Aldeen M. Robust overlapping load frequency output feedback control of multi-area interconnected power systems. Int. J. Electrical Power and Energy Systems, 2017, **89**, pp.156–172.

[5] Mbungu N. T., Naidoo R. M., Bansal R. C., et al: An overview of renewable energy resources and grid integration for commercial building applications. Journal of Energy Storage, 2020, **29** pp. 101385.

[6] Saxena S., Hote Y. V.: Decentralized PID load frequency control for perturbed multi-area power systems. Int. J. Electrical Power and Energy Systems, 2016, **81**, pp. 405- 415.

[7] Pahasa J., Ngamroo I.: PHEVs Bidirectional Charging/Discharging and SoC Control for Microgrid Frequency Stabilization Using Multiple MPC. IEEE Trans. Smart Grid, 2015, **6**, (2), pp. 526-533.

[8] Tungadio D. H., Bansal R. C., Siti M. W., et al.: Predictive Active Power Control of Two Interconnected Microgrids. Tech. Econo. Smart Grid and Sust. Energy, 2018, **3**, (3), pp. 1–15.

[9] Yousef H., AL-Kharusi K., Albadi M., et al.: Load frequency control of a multi-area power system: An adaptive fuzzy logic approach. IEEE Trans. Power Syst., 2014, **29**, (4), pp. 1822–1830.

[10] Mbungu, N. T., Naidoo, R., Bansal, el al.: Optimization of grid connected hybrid photovoltaic–wind–battery system using model predictive control design', IET Renewable Power Generation, 2017, **11**, (14), pp. 1760-1768.

[11] Tungadio, D. H., Bansal, R. C., and Siti, M. W.: Energy flow estimation-control of two interconnected microgrids. Journal of Energy in Southern Africa, 2018, **29**, (4), pp. 69-80.

[12] Mbungu, N. T., Bansal, R. C., Naidoo, R. M., et al.: Analysis of a grid-connected battery energy storage based energy management system. IEEE in First International Conference on Power, Control and Computing Technologies (ICPC2T), 2020, pp. 1-5.

[13] Bansal R. C.: Automatic reactive power control of autonomous hybrid power systems. PhD thesis, IIT Delhi, India, 2003.

[14] Mbungu, N. T.: Dynamic real time electricity pricing optimization for commercial building. MEng: Department of Electrical, Electronic and Computer Engineering, University of Pretoria, South Africa, 2017.

[15] McNamara P., Negenborn R. R., De Schutter B., et al.: Optimal coordination of a multiple HVDC link system using centralized and distributed control. IEEE Trans. Control Syst. Technol., 2013. **21**, (2), pp. 302–314.

[16] Mbungu N.T., Bansal R.C., Naidoo R., et al.: An optimal energy management system for a commercial building with renewable energy generation under real-time electricity prices. Sust. Cit. Soc. 2018; **41**, 392–404.

[17] Chowdhyry A., Asaduzzaman M..: Load Frequency of multigrid using Energy storage system. Conference on Electrical and computer Engineering 20-22 Dec. 2014.

[18] Siti M. W., Nicolae D. V., Jimoh A. A., et al.: Reconfiguration and load balancing in the LV and MV distribution networks for optimal performance. IEEE Trans. Power Deliv., 2007, **22**, (4), pp. 2534–2540.

[19] Mbungu N.T., Bansal R.C., Naidoo R.M., et al.: A dynamic energy management system using smart metering. Applied Energy, **280**, pp. 115990..

[20] Chen S. X., Gooi H. B., Xia N., et al.: Modelling of lithium-ion battery for online energy management systems. *IET Electrical Systems in Transportation*, 2012, **2**, (4), pp. 202-210.

[21] Tungadio D. H., Bansal R. C., and Siti M.W.: Optimal control of active power of two micro-grids interconnected with two AC tie-lines. Electric Power Components and Systems, 2017, **45**, (19), pp. 2188-2199.

[22] Mbungu, N. T., Bansal, R. C., and Naidoo, R. M.: Smart energy coordination of autonomous residential home. IET Smart Grid, 2019, **2**, (3), pp. 336-346.

[23] Bansal R.C.: Handbook of Distributed generation: Electric Power Technologies, Economics and Environmental Impacts, Springer, Cham, Switzerland, 2017.

[24] Mbungu, N. T.: Smart energy coordination for a microgrid. PhDEng: Department of Electrical, Electronic and Computer Engineering, University of Pretoria, South Africa, 2020.